



**University of
Zurich**^{UZH}

**Zurich Open Repository and
Archive**

University of Zurich
University Library
Strickhofstrasse 39
CH-8057 Zurich
www.zora.uzh.ch

Year: 2015

Contribution of the incudo-malleolar joint to middle-ear sound transmission

Gerig, Rahel ; Ihrle, Sebastian ; Rösli, Christof ; Dalbert, Adrian ; Dobrev, Ivo ; Pfiffner, Flurin ;
Eiber, Albrecht ; Huber, Alexander M ; Sim, Jae Hoon

Abstract: The malleus and incus in the human middle ear are linked by the incudo-malleolar joint (IMJ). The mobility of the human IMJ under physiologically relevant acoustic stimulation and its functional role in middle-ear sound transmission are still debated. In this study, spatial stapes motions were measured during acoustic stimulation (0.25-8 kHz) in six fresh human temporal bones for two conditions of the IMJ: (1) normal IMJ and (2) IMJ with experimentally-reduced mobility. Stapes velocity was measured at multiple points on the footplate using a scanning laser Doppler vibrometry (SLDV) system, and the 3D motion components were calculated under both conditions of the IMJ. The artificial reduction of the IMJ mobility was confirmed by measuring the relative motion between the malleus and the incus. The magnitudes of the piston-like motion of the stapes increased with the reduced IMJ mobility above 2 kHz. The increase was frequency dependent and was prominent from 2 to 4 kHz and at 5.5 kHz. The magnitude ratios of the rocking-like motions to the piston-like motion were similar for both IMJ conditions. The frequency-dependent change of the piston-like motion after the reduction of the IMJ mobility suggests that the IMJ is mobile under physiologically relevant levels of acoustic stimulation, especially at frequencies above 2 kHz.

DOI: <https://doi.org/10.1016/j.heares.2015.07.011>

Posted at the Zurich Open Repository and Archive, University of Zurich

ZORA URL: <https://doi.org/10.5167/uzh-112223>

Journal Article

Accepted Version



The following work is licensed under a Creative Commons: Attribution-NonCommercial-NoDerivatives 4.0 International (CC BY-NC-ND 4.0) License.

Originally published at:

Gerig, Rahel; Ihrle, Sebastian; Rösli, Christof; Dalbert, Adrian; Dobrev, Ivo; Pfiffner, Flurin; Eiber, Albrecht; Huber, Alexander M; Sim, Jae Hoon (2015). Contribution of the incudo-malleolar joint to middle-ear sound transmission. *Hearing research*, 327:218-226.

DOI: <https://doi.org/10.1016/j.heares.2015.07.011>

CONTRIBUTION OF THE INCUDO-MALLEOLAR JOINT TO MIDDLE-EAR SOUND TRANSMISSION

¹Rahel Gerig*, ²Sebastian Ihrle, ¹Christof Rösli, ¹Adrian Dalbert, ¹Ivo Dobrev, ¹Flurin Pfiffner,
²Albrecht Eiber, ¹Alexander M. Huber, ¹Jae Hoon Sim

¹University Hospital Zurich, University of Zurich, ²University of Stuttgart

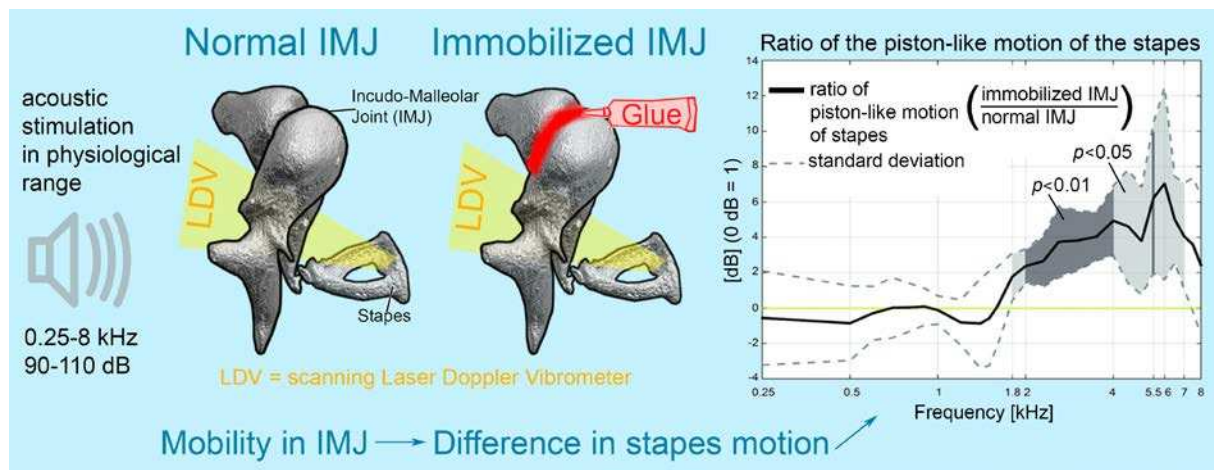
*Corresponding author e-mail address: MEM_ENT@usz.ch

Abstract

The malleus and incus in the human middle ear are linked by the incudo-malleolar joint (IMJ). The mobility of the human IMJ under physiologically relevant acoustic stimulation and its functional role in middle-ear sound transmission are still debated. In this study, spatial stapes motions were measured during acoustic stimulation (0.25-8 kHz) in six fresh human temporal bones for two conditions of the IMJ: (1) normal IMJ and (2) IMJ with experimentally-reduced mobility. Stapes velocity was measured at multiple points on the footplate using a scanning laser Doppler vibrometry (SLDV) system, and the 3D motion components were calculated under both conditions of the IMJ. The artificial reduction of the IMJ mobility was confirmed by measuring the relative motion between the malleus and the incus. The magnitudes of the piston-like motion of the stapes increased with the reduced IMJ mobility above 2 kHz. The increase was frequency dependent and was prominent from 2-4 kHz and at 5.5 kHz. The magnitude ratios of the rocking-like motions to the piston-like motion were similar for both IMJ conditions. The frequency-dependent change of the piston-like motion after the reduction of the IMJ mobility suggests that the IMJ is mobile under physiologically relevant levels of acoustic stimulation, especially at frequencies above 2 kHz.

Keywords: Incudo-malleolar joint (IMJ); incudo-malleal joint (IMJ); malleo-incudal joint; incudo-mallear joint; articulatio incudomallearis; middle ear; malleus; incus; stapes; piston-like motion; rocking-like motion; Laser Doppler Vibrometer (LDV); micro-CT

Abbreviations: **3D**: three dimensional; **AEC**: artificial ear canal; **IMJ**: incudo-malleolar joint; **ISJ**: incudo-stapedial joint; **LDV**: laser Doppler vibrometry; **Micro-CT**: micro-computed tomography; **SLDV**: scanning laser Doppler vibrometry; **TB**: temporal bone; **TM**: tympanic membrane



1. Introduction

The ossicular chain in the human middle ear transmits sound-induced mechanical vibrations of the tympanic membrane (TM) to the inner ear. The middle-ear ossicular chain comprises three bones -- the malleus, incus, and stapes, which are connected via the incudo-malleolar joint (IMJ) and incudo-stapedial joint (ISJ).

The IMJ connects the articular surfaces of the malleus and incus and has a twisted saddle shape (Helmholtz 1863; Etholm and Belal, 1974; Sim and Puria, 2008). It has previously been described in the literature as a synovial joint (diarthrodial joint/diarthrosis) (Politzer, 1884; Harty, 1953, 1964; Etholm and Belal, 1974; Schuknecht, 1974; Marquet, 1981; Hüttenbrink and Pfausch, 1987; FICAT, 1998; Sim and Puria, 2008). According to the literature, the IMJ is encapsulated by fibrous structures along its borders and contains synovial fluid inside the capsule, without the muscular components that are present in skeletal joints. The thickness of the IMJ tissue structures between the articular surfaces of the malleus and the incus varies from 0.04 mm to 0.32 mm along the intra-articular space, with maximal thickness on the medial and lateral aspects (Sim and Puria, 2008). The anatomical features of the IMJ may allow it to be deformed, resulting in relative motions between the malleus and incus.

The role of the IMJ as a protection mechanism against large static pressure changes has been proposed. For example, Kirikae (1960) argued that the IMJ is immobile up to 140 dB SPL, after which relative motion between the malleus and the incus could occur. Hüttenbrink (1988a) found that the IMJ is mobile under static pressure change. Such relative shear motions between the malleus and incus in human temporal bones (TBs) has been found in other studies as well (Kobrak, 1959; Cancura, 1980; Hüttenbrink, 1988b; Dahmann, 1929; Politzer, 1873; Mach and Kessel, 1874).

While relative displacement between the malleus and the incus under static pressure change of large magnitudes is generally accepted, flexibility of the human IMJ under acoustic

stimulation at physiologically-relevant levels and its functional role in middle-ear sound transmission are still under debate.

Several previous works have proposed frequency-dependent behavior of the IMJ, which allows considerable relative motion between the malleus and incus only for the high frequencies. Elpern et al. (1965) observed relative motion above 4 kHz in human TBs, Guinan and Peake (1967) more relative motions at "higher frequencies" in cats and Willi et al. (2002) above 2 kHz in human TBs. Such high-frequency dominant slippage was also observed in three-dimensional measurements of ossicular motion in one human TB (Decraemer and Khanna, 2004). "Slippage" of the IMJ was observed in a study with two human TBs even for the low frequencies (Decraemer and Khanna, 2001), but in their study, the slippage was dominant at the high frequencies.

While some previous studies have argued that the IMJ is functionally immobilized during middle-ear sound transmission under physiological acoustic stimulation, the methods used in these studies did not account for factors that we realize today can influence the results resulting in potential inaccuracies. Harty (1964) made predictions based solely on morphological examination. Békésy (1960) used TBs with a drained cochlea in his measurements. It is known that absence of impedance of the cochlear fluid with a drained cochlea results in an increase of the middle-ear transfer function, especially above 0.5 kHz (Gyo et al. 1987). Some measurement systems were in contact with the middle-ear ossicles, which may change the natural motions of the ossicles. One example is a capacitive probe (Békésy, 1941), where a piece of metal foil is attached to measure the vibration of the surface of interest. Gundersen and Hogmoen, (1976) performed their measurements only at frequencies below 2 kHz with time-averaged holographic methods. The measurement with an electromagnetic probe in a study reported by Cancura (1980) was only static and not dynamic. In Elpern et al. (1965), the immobilization of the IMJ was not verified; thus the information of the degree of immobilization was missing.

Willi (2003) and Offergeld et al. (2007) have reported that relative motion between the malleus and the incus caused by the mobility of the IMJ resulted in frequency-dependent transmission loss in the middle-ear transfer function. Willi (2003) observed that immobilizing the IMJ resulted in less transmission loss between the malleus and incus. In this study, after the immobilization of the IMJ, almost no change in transmission was observed below 1.5 kHz, and the transmission increased with frequency above 3 kHz, reaching a 10-dB increase at 10 kHz. Similarly, an increase (less than 10 dB) of stapes motion amplitude occurred in the high frequencies (from 1.2 kHz to 5 kHz) after immobilization of the IMJ, as reported by Offergeld et al. (2007). However, the work by Willi explored transmission loss between the malleus and incus rather than transmission loss through the entire middle ear, which is defined as motion of the stapes with respect to ear-canal pressure. Further, the measurements and analysis were two-dimensional. In the work by Offergeld et al., motions of the stapes were measured one-dimensionally, and immobilization of the IMJ was not quantitatively examined.

In our study, it is hypothesized based on previous studies that the IMJ is mobile under physiological relevant acoustic stimulation, and the mobility of the IMJ results in transmission loss in the middle-ear transfer function, especially at higher frequencies. Our aim is to assess the contribution of the IMJ to middle-ear sound transmission accurately by using current methodologies that include quantification of artificial immobilization of the IMJ and three-dimensional measurement of stapes motion.

2. Material and Methods

Fresh TBs from human cadavers were used in this study, and approval was obtained by the Ethical Committee of Zurich (KEK-ZH-Nr. 2012-0007).

To assess the contribution of the IMJ to middle-ear sound transmission in human ears, spatial motions of the stapes, which were measured using a laser Doppler vibrometry (LDV) system, were compared under two different conditions of the IMJ: (1) normal IMJ and (2) IMJ with experimentally reduced mobility. To reduce the mobility of the IMJ, the articular capsule of the IMJ was opened with a surgical hook on the superior side, and removal of the synovial liquid was facilitated by capillary flow to an absorbent tissue. Then, the cavity was filled with glue (Denseal Superior, Prevest Denpro GmbH, Germany) such that the glue replaced the synovial fluid and connected the articular surfaces of the malleus and the incus. For purposes of the study, we refer to the unmodified IMJ as “mobile IMJ,” and the IMJ with reduced mobility following insertion of the glue (reduced by 15-18 dB, see Fig. 3) as “immobilized IMJ.”

The effectiveness of the immobilization of the IMJ was quantified based on the relative motions between the malleus and incus, measured on an area covering the superior parts of the malleus head and the incus body around the IMJ using the LDV system. Once the immobilization was confirmed, spatial motions of the stapes were re-measured and compared to corresponding data with the mobile IMJ. To avoid bias due to physiological changes of middle-ear tissues caused by drying (Rosowski et al., 1990; Voss et al., 2000; Sim et al., 2004), the samples were placed in saline solution for 30 minutes prior to the second stage of the measurement, which was with the immobilized IMJ. The time interval between removing the TBs from the saline solution and the measurements was kept constant at approximately 20 minutes for both stages of the measurement.

2.1 Temporal Bone Preparation

The fresh TBs were harvested within 24 hours after death and were preserved in thiomersal 0.1 % (thimerosal, $C_9H_9HgNaO_2S$) solution at 4° C. Subsequent measurements were done within 7 days after the TBs were harvested (except for TB 2, which was done at 13 days). One TB, which did not conform with the American Society for Testing and Materials (ASTM) standard (F2504-05, Philadelphia, 2005), was excluded during the first stage of the measurements, resulting in a total of six TBs. The six fresh TBs were from four males and two females, with an average age of 68.2 years (ranging from 48 to 83 years).

Exposure of the middle-ear ossicular chain, which included a near-perpendicular view of the stapes footplate and a superior-medial view of the malleus-incus complex, was made by a mastoidectomy with posterior tympanotomy. The TM, middle-ear ossicles, ligaments, and tendon were left intact. The external ear canal was removed and was replaced by an artificial ear canal (AEC) of about 0.5-ml volume (diameter of 9.65 mm and length of 6-8 mm) (Sim et al., 2010, 2012; Lauxmann et al., 2012).

2.2 Acoustical stimulation and measurements of ossicular motion

The stapes motions were measured with harmonic excitations at 26 different frequencies in the range of 0.25 to 8 kHz. The excitation signals were provided by a signal generator incorporated within the PSV data acquisition system (Polytec GmbH, Germany). The stimulation, amplified by an amplifier (RMX 850, QSC Audio Products, USA), was delivered by a loudspeaker (ER-2, Etymotic Research, USA) embedded in the AEC. The sound pressure level (SPL) in the AEC was in the range of 90 – 110 dB SPL, measured by a microphone probe (ER-7C, Etymotic Research, USA).

To obtain the spatial components of the stapes motion, velocities at multiple points (approximately 100 points) on the stapes footplate were measured by a scanning laser Doppler vibrometry (SLDV) system (OFV-3001 SLDV system, Polytec GmbH, Germany). To improve the signal-to-noise ratio of the SLDV, retro-reflective glass beads (50 microns)

were attached to the stapes footplate. A video camera (VCT 24), oriented coaxially with the laser beam, was used to determine the measurement area on the footplate as well as the 2D coordinates (i.e., X and Y coordinates) of the measurement points in the SLDV measurement frame (corresponds to XYZ coordinate system in Fig. 1). In the SLDV measurement frame, the XYZ coordinate system was set such that the laser beam was along the Z direction and the XY plane was normal to the laser beam. The angle θ between the laser beam direction (i.e., Z axis of SLDV frame) and the z axis of the anatomical frame (see Fig. 1) was $34 \pm 11^\circ$.

The mobility of the IMJ was monitored before and after immobilization. Motions of the malleus and incus were measured from a superior-medial view at about 150 points, covering areas on the malleus head and incus body adjacent to the IMJ. The number of measurement points for the malleus and the incus were approximately equal. The acoustic stimulation was by harmonic signals at 0.5, 1, 2, 4, and 6 kHz, in the range of 90 – 110 dB SPL where motions of the human middle-ear ossicular chain as a function of stimulation level are presumed to be linear (Schön and Müller, 1999).

All measurement procedures were controlled by PSV V9.0 software (Polytec GmbH, Germany), and were automated by a custom-made macro within the PSV V9.0 software.

2.3 Registration into anatomical frame (footplate-fixed frame)

After the two stages of the motion measurements of the stapes, all the temporal bones were imaged using the micro-CT 40 (SCANCO Medical AG, Switzerland), with resolutions of 15-18 μm . The 3D features of the stapes were reconstructed from the micro-CT images, and the footplate-fixed anatomical frame (corresponds to xyz coordinate system in Fig. 1) of each temporal bone was obtained, such that the xy -plane was fitted to the median surface of the corresponding stapes footplate, and the origin was located at the centroid of the median surface. The anterior direction was set as the positive x -direction, the superior direction as the positive y -direction, and lateral direction as the positive z -direction. Thereby, a right-handed

frame system was made for the right ear (Fig. 1) and a left-handed frame system for the left ear.

To correlate XYZ coordinates in the SLDV measurement frame with xyz coordinates in the footplate-fixed frame, four or five reference markers (copper wires of 0.75-mm diameter) were glued to the peripheral bones, and the XY coordinates of their outlines in the SLDV measurement frame were recorded. The 3D features of the reference markers were also obtained from micro-CT images, and the correlation between the two frames was calculated such that the outline of the reference markers recorded in the SLDV measurement frame was fitted to the outline of the 3D features from the micro-CT images. Once the correlation between the two frames was obtained, the measurement points and measured velocities at those points in the SLDV measurement frame were registered into the footplate-fixed frame, in order to calculate the 3-D motion components of the stapes in the footplate-fixed frame. Details of the frame registration procedures have been described previously (Sim et al., 2010, 2012).

2.4 Transfer function of the middle ear

Spatial motion components of the stapes were calculated by a method that we have used previously (Sim et al., 2010), in which the translation of the footplate's center along the medial-lateral direction (z -direction; piston-like motion, V_{oz}) and two rotations about the long (x -direction) and short (y -direction) axes of the footplate (rocking-like motions) were considered as the dominant rigid-body motion components of the stapes (Lauxmann et al., 2012). Consequently, the velocities of the three rigid-body motion components were normalized by the measured ear-canal pressure to obtain the corresponding transfer-function components.

2.5 Quantification of the IMJ mobility

To quantify the relative motion between the malleus and the incus before and after the IMJ immobilization, the relative motion around the IMJ was measured from a superior view, and the magnitude ratios of the relative motion components to the corresponding motion components of the malleus and incus (R_{VO} , $R_{\omega X}$, $R_{\omega Y}$, and R_{TOTAL}) were obtained.

The SLDV system was positioned for the right ear such that the approximate alignments of the direction of each axis were: the X -axis, posterior-to-anterior; the Y -axis, lateral-to-medial; the Z -axis, the inferior-to-superior. Since the motions of the malleus and the incus were measured with only one laser beam direction, only three rigid-body motion components for each of the malleus and incus could be obtained in the SLDV measurement frame: translation along the laser beam direction (Z -direction) and two rotations about the X - and Y -axes of the SLDV measurement frame (Note that the SLDV measurement frame here has nothing to do with either the SLDV measurement frame or the anatomical frame in stapes motion shown in Fig. 1). The translational motion along the laser beam direction was calculated with respect to the center of the measurement area (denoted as O), which was located on the IMJ, for both the malleus and the incus. Next, the relative motions in the three rigid body motion components were calculated by

$$\begin{aligned} |V_{OR}| &= |V_{OM} - V_{OI}|, \\ |\omega_{XR}| &= |\omega_{XM} - \omega_{XI}|, \\ |\omega_{YR}| &= |\omega_{YM} - \omega_{YI}|, \end{aligned} \tag{1}$$

where V_{OM} , ω_{XM} , and ω_{YM} are the translational velocity of the point O along the laser beam direction and two rotational velocities for the malleus, V_{OI} , ω_{XI} , and ω_{YI} are the translational velocity of the point O along the laser beam direction and two rotational velocities for the incus, and V_{OR} , ω_{XR} , and ω_{YR} are the corresponding relative velocities. In calculation of Eq. (1), all the velocity components were treated as complex numbers to consider the phases. Then, each relative motion component was normalized by the magnitude of the corresponding

motion component of the malleus and incus, as an index representing the ratio of the relative motion to motion of the malleus and incus (R_{vO} , $R_{\omega X}$, and $R_{\omega Y}$).

$$R_{vO} = \frac{|V_{OR}|}{(|V_{OM}| + |V_{OI}|)/2},$$

$$R_{\omega X} = \frac{|\omega_{XR}|}{(|\omega_{XM}| + |\omega_{XI}|)/2},$$

$$R_{\omega Y} = \frac{|\omega_{YR}|}{(|\omega_{YM}| + |\omega_{YI}|)/2}. \quad (2)$$

In Eq. (2), the magnitudes of the corresponding motion components of the malleus and incus were obtained as the average of magnitudes of the malleus motion components and the incus motion components. To represent the ratio of the total relative motion to the incus and malleus motion, the ratios of the relative motion components were averaged with the ratio components weighted by portions of the corresponding motion components.

$$R_{TOTAL} = W_{vO} R_{vO} + W_{\omega X} R_{\omega X} + W_{\omega Y} R_{\omega Y}, \quad (3)$$

In Eq. (3), W_{vO} , $W_{\omega X}$, and $W_{\omega Y}$ indicate weighting coefficients of $|V_{OR}|$, $|\omega_{XR}|$, and $|\omega_{YR}|$, which are calculated by portions of the corresponding motion components.

$$W_{vO} = \frac{|V_{OM}| + |V_{OI}|}{D},$$

$$W_{\omega X} = \frac{|\omega_{XM}| \cdot |\bar{Y}_M| + |\omega_{XI}| \cdot |\bar{Y}_I|}{D},$$

$$W_{\omega Y} = \frac{|\omega_{YM}| \cdot |\bar{X}_M| + |\omega_{YI}| \cdot |\bar{X}_I|}{D},$$

with $D = (|V_{OM}| + |V_{OI}|) + (|\omega_{XM}| \cdot |\bar{Y}_M| + |\omega_{XI}| \cdot |\bar{Y}_I|) + (|\omega_{YM}| \cdot |\bar{X}_M| + |\omega_{YI}| \cdot |\bar{X}_I|)$,

where $|\bar{Y}_M|$ and $|\bar{Y}_I|$ are average distances of measurement points from the center point O in the Y direction, and $|\bar{X}_M|$ and $|\bar{X}_I|$ are average distances of measurement points from the center point O in the X direction, for the malleus and the incus. The multiplication of the

average distances to the magnitudes of the corresponding rotational velocity components was done in order to make the magnitudes of the rotational velocity components equivalent to the magnitudes of the translational velocity components.

2.6 Statistical analysis

Frequency-dependence and age-dependence of the normal IMJ mobility were analyzed using an ANOVA for repeated measures (with age as covariate for examination of age dependence). Frequency-dependence and age-dependence of the relative change of the piston-like motion between the mobile and immobilized conditions of the IMJ were also analyzed using an ANOVA for repeated measures (with age as covariate for examination of age dependence), with the two variables as the IMJ condition (i.e., mobile and immobilized) and frequency. Data were logarithmically transformed for this analysis. Deviations from sphericity were addressed using the Greenhouse-Geisser correction. Post-hoc comparison with paired *t*-tests was performed for comparison between the mobile and immobilized conditions of the IMJ at each frequency. The statistical calculations were done with SPSS 20 software (IBM, USA).

3. Results

3.1 Drying Effect

Figure 2 depicts changes of the motion of the stapes (footplate center) due to drying of the TB tissues. The drying effects were examined in an additional TB, and this TB was not used in the further experiments of the study. The drying effects shown in Fig. 2 are presumed to be similar for all temporal bones. The sample was immersed for 30 minutes in saline solution, and the first measurement (0 min in the figure) took place within 5 minutes after removal from the saline solution. There is a trend for the first natural frequency to increase with time, indicating a stiffening of the suspensory structures due to the drying. The clear phase shift with drying was observed as well. Consequently, over time, there is a reduction in the magnitudes of motions at frequencies below the resonance and an increase of motions above the resonance. The change in the lower frequencies between 90 – 150 minutes of drying was larger than the change during other time intervals. The changes for the higher frequencies were also minimized after 150 minutes. Then, the sample was re-hydrated by immersion in the saline solution for 30 minutes, and the measurement was repeated within 5 minutes after removal from the saline solution ('Rehydration' in the figure). The magnitude of the motion of the stapes with rehydration recovered to approximately the same levels as before drying.

3.2 Immobilization of the IMJ

Figure 3 displays the index for the ratios of the relative motion components between the malleus and the incus to the corresponding motion components of the malleus and incus, calculated using Eqs. (1) - (3), before (solid) and after (dashed) the IMJ was immobilized. Before the IMJ was immobilized, the averaged relative motion ratios (R_{TOTAL}) were small in the low frequency range (-17.5 ± 2.9 dB at 0.5 kHz), and increased with frequency, reaching 0.1 ± 1.9 dB at 6 kHz. The relative motion ratio of $\omega_Y (R_{\omega Y})$ was larger than the relative motion

ratios of the other components, but its contribution to the weighted average ratio (R_{TOTAL}) was smaller than the contribution of the relative motion ratios of the other components because the motion components ω_{YM} and ω_{YI} of the malleus and incus had smaller magnitudes than other motion components (i.e., $W_{\omega Y}$ was smaller than W_{vO} and $W_{\omega X}$). No dependence of the relative motion on age was observed with the six temporal bones used in this study (ANOVA with age as covariate). After the IMJ was immobilized, the averaged relative motion ratios were reduced by 10 to 15 dB (i.e., R_{TOTAL} was reduced to 18 – 30 % of the values before immobilization of the IMJ), along the frequency range of 0.5 – 6 kHz ($p < 0.05$ at 1 kHz and $p < 0.01$ at all other frequencies with paired t -test). The immobilization of the IMJ was more effective for higher frequencies, where the IMJ had more relative motion before the immobilization (R_{TOTAL} was reduced by 10 dB at 0.5 kHz and by 15 dB at 6 kHz).

3.3 Stapes Motion Before/After the IMJ Immobilization

Figure 4 illustrates the magnitude of the translational motions of the footplate's center along the z -axis (i.e., piston-like motions, V_{oz}) normalized by the ear canal pressure, before (solid) and after (dashed) the IMJ was immobilized, for all six temporal bones used in this study (TB1-TB6).

To determine the effect of the IMJ immobilization on the translational motions, changes of the translational motion with immobilized IMJ relative to the translational motion with mobile IMJ were calculated, and the results are shown in Fig. 5 (relative magnitude ratios (left) and relative phase difference (right)). In the figure, the relative change was calculated for each temporal bone, then the relative changes were averaged over all the temporal bones ($n = 6$). An ANOVA for repeated measures on the magnitude change revealed that the difference of the magnitude between the two IMJ conditions was frequency-dependent ($p = 0.004$). While the magnitudes were similar for both IMJ conditions at frequencies below 1.8 kHz, the magnitudes were generally higher for the immobilized IMJ for

the higher frequencies. The paired *t*-test resulted in *p*-values less than 0.05 for frequencies in the 1.8 to 7 kHz range and *p*-values less than 0.01 for frequencies from 2 to 4 kHz and at 5.5 kHz (shaded with dark gray in Fig. 5). The immobilization of the IMJ also tended to cause an increase in phase between 1.5 and 4 kHz. Because of the age range of the TBs and the proposition that mobility could change as a function of age, we examined dependence of the results on age, and no dependence of the relative change on age was observed (ANOVA with age as covariate).

To observe the changes in magnitude ratios of the two rotational velocities (i.e., rocking-like motions) relative to the translational velocities of the footplate-center (i.e., piston-like motion) following immobilization of the IMJ, the linear velocities at the inferior and posterior edges of the footplate generated by the two rotational velocities were calculated, and were normalized by the footplate-center velocity in the *z*-direction (Heiland et al. 1999; Hato et al. 2003; Sim et al. 2010), for mobile and immobilized IMJ conditions (Fig. 6). The mean values and corresponding standard deviations for each of the mobile and immobilized IMJ conditions were calculated after the relative ratios were obtained for each of the temporal bones (*n* = 6). The inferior-edge velocities were calculated by multiplication of half of the footplate's short length to the rotational velocity components along the long axis of the footplate, and the posterior-edge velocities by multiplication of half of the footplate's long length to the rotational velocity components along the short axis of the footplate (Sim et al., 2010). The short and long lengths of the footplate were measured from the reconstructed shapes of the stapes, which were obtained from micro-CT imaging for each of the temporal bones. The lengths were 2.86 ± 0.250 mm along the long axis and 1.40 ± 0.101 mm along the short axis, and were slightly longer than the lengths of specimens used in Sim et al. 2013 (2.81 ± 0.158 mm along the long axis and 1.27 ± 0.109 mm along the short axis).

The mean ratio of the inferior-edge velocity to the footplate-center velocity was approximately -18 dB at 0.25 kHz and increased with frequency, for the both mobile (solid)

351 and immobilized IMJ (dashed) conditions. The trends were similar for the ratio of the
352 superior-edge velocity to the footplate-center velocity. While Fig. 6 shows the ratios of the
353 edge velocities to the footplate-center velocity separately for each of the mobile and
354 immobilized IMJ conditions, post-hoc comparison with paired *t*-tests was performed for
355 comparison of the ratios between the mobile and immobilized IMJ conditions. No significant
356 difference between the mobile and immobilized IMJ conditions was observed for either the
357 ratio of the inferior-edge velocity to the footplate-center or the ratio of the superior-edge
358 velocity to the footplate-center velocity.

4. Discussion

The goal of this study was to investigate the role of the IMJ in middle-ear sound transmission under physiologically-relevant acoustic stimulation. We controlled for bias due to a drying effect of the TBs in two ways. Each specimen was periodically moistened during the measurements, and the specimens were placed in a saline solution for 30 minutes prior to the measurement with the immobilized IMJ. Previous studies (Rosowski et al. 1990; Voss et al., 2000; Willi et al., 2002; Sim et al., 2004) have reported that physiological changes of the middle-ear tissues due to drying result in significant increase of the resonant frequency of the middle-ear ossicular chain. These studies have also found that the shift of the resonant frequency accelerates with time during a couple of hours at the beginning. Voss et al. (2000) have argued that measurements with TBs are typically presumed to be stable for a "couple of hours," but there is large variability across TBs in the rate of acceleration of the physiological changes of the middle-ear tissues. Our examination of the drying effect (Fig. 2) shows similar trends. We also found that the effect can be reversed by immersing the TBs in saline solution, thus the motion of the stapes recovers to approximately the same levels as before being dried. Such restoration of the mechanical properties of the middle-ear tissues by immersing the TBs in saline solution has been observed in other studies (Voss et al., 2000; Willi et al., 2002; Nakajima et al., 2005).

Artificial immobilization of the IMJ in this study was performed under the microscope by applying glue to the inner space of the IMJ capsule after removal of the synovial fluid. The effectiveness of the artificial immobilization procedures was confirmed by measurements of the relative motion between the malleus and incus before and after the artificial immobilization (Fig. 4). The relative motion was reduced by 10 to 15 dB after the artificial immobilization.

Our results indicate that a mobile IMJ attenuates the magnitude of middle-ear sound transmission, especially for frequencies above 2 kHz. The mean piston-like motion (V_{oz})

increases after immobilization by less than 7 dB for the frequencies from 1.8 to 8 kHz. Specifically, the prominent difference occurs from 2 to 4 kHz, and at 5.5 kHz ($p < 0.01$ with paired t -test). With the mobile IMJ, the ratios of the two rocking-like motions to the piston-like motion were frequency-dependent ($p < 0.001$ with ANOVA test), that is to say, there were relatively large rocking-like motions at higher frequencies. This is in agreement with results from previous studies (Heiland et al., 1999; Hato et al., 2003; Sim et al., 2010). The two ratios showed no significant difference between the mobile and immobilized IMJ conditions, suggesting that there are no important changes in relative magnitude ratios of the rocking-like motions to the piston-like motion caused by immobilization of the IMJ.

The larger difference of the piston-like stapes motion between the mobile and immobilized IMJ conditions at higher frequencies is presumed to be due to relatively large loss of motion from malleus to incus at higher frequencies for the normal IMJ as compared to the immobilized IMJ. With the normal condition of the IMJ (i.e., before the IMJ immobilization), the index for the ratio of the relative motion (R_{TOTAL}) increased with frequency (Fig 3), indicating more relative motion at higher frequencies. Therefore, the mobility of the IMJ will not affect the middle-ear sound transmission at low frequencies considerably. At frequencies above 4 kHz, the R_{TOTAL} is maximized and reaches almost 0 dB (i.e., ratio of 1), indicating that the magnitude of the relative motion is almost the same as the average magnitude of the malleus motion and the incus motion. Therefore, in this frequency range, the immobilization of the IMJ is expected to affect the middle-ear transmission significantly.

The high-frequency dominant change in middle-ear sound transmission due to mobility of the IMJ in human TBs has been described previously. Huber et al. (1997) reported a transmission loss from the malleus to the incus of about 6 dB at frequencies above 2 kHz under acoustic stimulation at moderate SPLs. Offergeld et al. (2007) observed an increase of less than 10 dB in the amplitude of the stapes motion after immobilization of the IMJ for

frequencies from 1.2 - 5 kHz. Willi et al. (2003) described that a decrease of 5.5 dB per octave above 1 kHz may be caused by the mobility of the IMJ, based on the transmission loss observed in his two-dimensional measurements of motions of the malleus and the incus.

Mobility of the human IMJ has been found in many previous studies (Helmholtz, 1868; Mach and Kessel, 1874; Frank, 1923; Dahmann, 1930; Stuhlman, 1937; Kobrak, 1959; Marquet, 1981; Schön and Müller, 1999; Huber et al., 1997; Decraemer and Khanna, 1999, 2001; Willi et al., 2002, 2003; Sim et al, 2004; Nakajima et al., 2005; Offergeld et al., 2007). Decraemer et al. (2014) also observed large slippage in the IMJ in TBs, and addressed two possible reasons for the slippage: 1) there are post-mortem changes in the cadaveric TBs that were used to examine the mobility of the IMJ in most studies; 2) the cadaveric TBs are from elderly people. They doubted that large slippage in the IMJ "really happens in the healthy living ear (pp. 508)".

It is known that cadaveric TBs have fast and slow post-mortem changes. The *fast* post-mortem changes, which are presumed to be caused mainly by a stoppage of blood flow and changes of the inner ear pressure in cadaveric ears, occur immediately after death (Brenkman and Grote, 1987). Békésy (1960), from his anatomical studies for human TBs, described that no considerable change of the elasticity of the ligaments, the joint capsule or the tympanic membrane occurs within several hours after death, indicating that the fast post-mortem changes probably do not affect middle-ear mechanics significantly. Several other studies have reported the fast post-mortem changes in animals as well, and found no considerable difference from living animals up to 1 hour in guinea pigs (Gilad et al. 1967), 1-2 hours in cats (Tonndorf and Khanna 1967, 1968), 17 hours in rabbits (Gill 1951), and 48 hours in rabbits (Onchi 1961).

The *slow* post-mortem changes, which may be caused by dehydration and autolysis, are important for the repeatability and stability of the measurements. According to previous studies, the slow post-mortem changes do not necessarily occur in all human TBs, and the

effects are not accentuated for a specific frequency range. Goode et al. (1993) measured umbo displacement 2 weeks and 4 weeks after death, and obtained almost the same frequency responses. Rosowski et al. (1990) observed considerable post-mortem changes before 100 days only in two out of nine TBs investigated. Brenkman and Grote (1987) observed from their measurement with two TBs that the umbo velocity was stable up to 45 hours after death and then decreased with post-mortem time for the investigated frequencies of 0.6, 2 and 5 kHz. Zwislocki and Feldman (1963) observed that the changes start in the low-frequency range. Effects of the slow post-mortem changes on the measurements in this study were unavoidable. However, they were minimized by preserving the fresh TBs in thiomersal 0.1 % solution at 4° C within 24 hours after death and by performing most measurements within a week after death (with the exception of TB2, which was measured 13 days after the death). No major differences in terms of stapes motion between live human subjects and fresh human TBs were obtained in intraoperative measurements (Huber et al. 2001, Chien et al. 2009), which strongly argues against large post-mortem effects. Therefore, our observation that the immobilized IMJ generates larger piston-like motions than the mobile IMJ only at frequencies above 2 kHz is not likely to be from the post-mortem changes of the TBs.

The fact that the temporal bones in this study are mostly from elderly subjects (average of 68 years) could have influenced the results. Although we did not observe an age dependency in our results, the number of samples is too small to draw a definitive conclusion. Decraemer and Khanna (2004) noted that their experiments also may have been biased due to use of temporal bones from elderly subjects. Willi (2003) describes a trend of a decrease of sound transmission at higher frequencies (> 3 kHz) with age in fresh human temporal bones, which would have to be confirmed in further measurements. Several morphological parameters of the IMJ may change with age including hyalinization or calcification of the joint capsule, thinning and calcification of the articular cartilage, thinning and calcification of the disc, and arthritis resulting in narrowing or obliteration of the joint space (Gussen, 1971;

Etholm and Belal, 1974). In addition, the amount of elastic fibers in the joint capsule tends to decrease with age (Harty, 1953), which may result in a reduction of the joint tension. Savić and Djerić (1988) describe degenerative changes in 40 % of their samples from persons between 40 and 60 years. While the reduction of the joint tension is expected to increase the mobility of the IMJ, effects of other morphological changes such as calcification and obliteration on the mobility of the IMJ have not been investigated, to our knowledge. With a possibility that the age-related morphological changes of the IMJ increase its mobility, we cannot rule out that the large mobility of the IMJ that we observed may have been due to the TBs from elderly people used in this study.

Another possibility is that the mobility of the IMJ exists as part of a protection mechanism, and the transmission loss at the high frequencies under moderate sound pressures is an unavoidable side effect of this mechanism. That is, the mobility of the IMJ that exists to protect the sensitive structures of the inner ear against high static pressure change also affects normal sound transmission with acoustic sound simulation of moderate levels. The protection mechanism has been proposed previously by several investigators (Dahmann, 1929, 1930; Békésy, 1936; Stuhlman 1937; Kobrak, 1959; Hüttenbrink, 1988a, 1988b, 1997; Cancura, 1980; Offergeld et al., 2000).

Puria and Steele (2010) predicted that the mobility of the IMJ could provide flexible adaptation to the complex motion of the malleus such as a twisting motion (i.e., rotational motion about the superior-inferior axis) at high frequencies. However, our results that artificial immobilization of the IMJ increased the middle-ear transfer function of the piston-like motion without change in the pattern of the stapes motion do not provide evidence for such a role of adaptation of the IMJ, at least up to 8 kHz, which is the frequency range considered in this study.

5. Conclusion

The IMJ was shown to be mobile at frequencies above 2 kHz under physiologically relevant acoustic stimulation of 90-110 dB SPL. A prominent frequency-dependent difference of the piston-like motion of the stapes between the mobile and immobilized IMJ conditions was observed; whereas, the ratio of the rocking-like motions relative to the piston-like motion of the stapes showed no significant difference. The prominent frequency-dependent change of the piston-like motion above 2 kHz is presumed to be due to large mobility of the IMJ at high frequencies. It is still questionable whether the mobility of the IMJ exists as part of a protection mechanism, regardless of age, or occurs only in elderly people due to aging effects. Since the sample size of six in this study is not sufficient to reveal the effects of age on middle-ear sound transmission, further measurements are required to clarify these open questions.

Acknowledgement

This study was funded by SNF (Swiss National Foundation) Project No. 138726 and by DFG (German Research Council) Project No. EI 231/6-1. The authors thank Prof. B. Seifert, Division of Biostatistics, Institute of Social- and Preventive Medicine, University of Zurich for the statistical consulting.

505 **References**

- 506 American Society for Testing and Materials (ASTM) F2504-05 (2005). Standard practice for
507 describing system output of implantable middle ear hearing devices. Philadelphia.
- 508 Békésy, von G., 1936. Zur Physik des Mittelohres und über das Hören bei fehlerhaftem
509 Trommelfell. Akust. Zeits. 1, 13–23.
- 510 Békésy, von G., 1941. Über die Messung Schwingungsamplitude der Gehörknöchelchen
511 mittels einer kapazitiven Sonde [About the vibration amplitude of the ossicles measured by
512 means of a capacitive probe] Akust Zeits. 6, 1–16.
- 513 Békésy, von G., 1960. Experiments in hearing. McGraw-Hill, New York.
- 514 Brenkman, C.J., Grote, J.J., 1987. Acoustic transfer characteristics in human middle ears
515 studied by a SQUID magnetometer method. J. Acoust. Soc. Am. 82, 1646-1654.
- 516 Cancura, W., 1980. On the statics of malleus and incus and on the function of the malleus-
517 incus joint. Acta Otolaryngol. 89 (3-4), 342-344.
- 518 Chien, W., Rosowski, J., J., Ravicz, M., E., Rauch, S., D., Smullen, J., Merchant, S., N., 2009.
519 Measurements of stapes velocity in live human ears. Hear. Res. 249, 54-61.
- 520 Dahmann, H., 1929. Zur Physiologie des Hörens; experimentelle Untersuchungen über die
521 Mechanik der Gehörknöchelchenkette, sowie über deren Verhalten auf Ton und Luftdruck.
522 Kongressbericht "zur Physiologie des Hörens". Z. Hals Nas. Ohrenheilkd. 24, 462-497.
- 523 Dahmann, H., 1930. Zur Physiologie des Hörens; Experimentelle Untersuchungen über die
524 Mechanik der Gehörknöchelchenkette sowie über deren Verhalten auf Ton und Luftdruck. Z.
525 Hals Nas. Ohrenheilkd. 27, 329-368.
- 526 Decraemer, W.F., Khanna, S.M., 1999. New insights in the functioning of the middle ear. In:
527 Rosowski, J.J., Merchant, S.N. (Eds.), The Function and Mechanics of Normal, Diseased and
528 Recon- structed Middle Ears. Kugler Publications, The Hague, 23-38.
- 529 Decraemer, W.F., Khanna, S.M., 2001. Complete 3-dimensional motion of the ossicular chain
530 in a human temporal bone. Abstract. Proceedings of the twenty-fourth Annual Midwinter
531 Research Meeting of the Association for Research in Otolaryngology 24, 221.
- 532 Decraemer, W.F., Khanna, S.M., 2004. Measurement, visualization and quantitative analysis
533 of complete three-dimensional kinematical data sets of human and cat middle ear. In: Gyo, K.,
534 Wada, H., Hato, N., Koike, T. (Eds.), Middle Ear Mechanics in Research and Otology. World
535 Scientific, Singapore. 3–10.
- 536 Decraemer W.F., Rochefoucauld O., Funnell W.R.J., Olson E.S., 2014. Three-dimensional
537 vibration of the malleus and incus in the living gerbil. Journal of the Association for Research
538 in Otolaryngology 15, 483-510.
- 539 Elpern, B.S., Greisen, O., Andersen, H.C., 1965. Experimental studies on sound transmission
540 in the human ear. VI. Clinical and Experimental Observations on Non-Otosclerotic Ossicle
541 Fixation. Acta Otolaryngol. 60 (1-6), 223-230.
- 542 Etholm, B., Belal, A., 1974. Senile changes in the middle ear joints. Ann. Otol. 83 (1), 49-54.
- 543 FICAT, 1998, Federative Committee on Anatomical Terminology (FICAT), International
544 Federation of Associations of Anatomists. Terminologia anatomica. Stuttgart: G. Thieme.

- 545 Frank, O., 1923. Die Leitung des Schalles im Ohr. Bayerische Akademie der Wissenschaften.
546 1923.
- 547 Gilad, P., Shtrikman, S., Hillmann, P., 1967. Application of the Mössbauer method to ear
548 vibrations. J. Acoust. Soc. Am. 41, 1232-1236.
- 549 Gill, N.W., 1951. Some observations on the conduction mechanism of the ear. J. Laryngol.
550 Otol. 65, 404-413.
- 551 Goode, R.L., Ball, G., Nishihara, S., 1993. Measurement of umbo vibration in human subjects
552 - method and possible clinical applications. Am J Otol. 103 (5), 565-569.
- 553 Gyo, K., Aritomo, H., Goode, R.L., 1987. Measurement of the ossicular vibration ratio in
554 human temporal bones by use of a video measuring system. Acta Otolaryngol. 103, 87-95.
- 555 Guinan, J.J., Peake, W.T., 1967. Middle-ear characteristics of anesthetized cats. J. Acoust.
556 Soc. Am. 41, 1237-1261.
- 557 Gundersen, T., Hogmoen, K., 1976. Holographic vibration analysis of the ossicular chain.
558 Acta Otolaryngol. 82, 16-25.
- 559 Gussen, R., 1971. The human incudomalleal joint. Chondroid articular cartilage and
560 degenerative arthritis. Arthritis Rheum. 14, 465-74.
- 561 Harty, M., 1953. Elastic tissue in the middle-ear cavity. The Journal of laryngology and
562 otology. 67, 723-729.
- 563 Harty, M., 1964. The joints of the middle ear. Z. Mikrosk. Anat. 71, 24-31.
- 564 Hato, N., Stenfelt, S., Goode, R.L., 2003. Three-dimensional stapes footplate motion in
565 human temporal bones. Audiol Neurotol. 8, 140-152.
- 566 Heiland, K.E., Goode, R.L., Asai, M., Huber, A.M., 1999. A human temporal bone study of
567 stapes footplate movement. AM J Otol. 20, 81-86.
- 568 Helmholtz, H. von, 1863. Die Lehre von den Tonempfindungen als physiologische Grundlage
569 für die Theorie der Musik, [On the Sensations of Tone as a Physiological Basis for the Theory
570 of Music], Sensations of Tone. J. Vieweg, Bayerische Staatsbibliothek.
- 571 Helmholtz, H. von, 1868. Die Mechanik der Gehörknöchelchenkette und des Trommelfells.
572 Pflüg. Arch. 1, 1-60.
- 573 Huber, A., Assai, M., Ball, G., Goode, R. L., 1997. Analysis of ossicular vibration in three
574 dimensions. In: Middle ear mechanics in research and otosurgery. Dresden. 82-87.
- 575 Huber, A., Linder, T., Ferrazzini, M., Schmid, S., Dillier, N., Stoeckli, S., Fisch, U., 2001.
576 Intraoperative assessment of stapes movement. Ann Otol Rhinol Laryngol. 110(1), 31-35.
- 577 Hüttenbrink, K.B., 1988a. Die Mechanik der Gehörknöchelchen bei statischen Drucken. I.:
578 Normales Mittelohr. Z. Laryngol. Rhinol. Otol. 67 (3), 45-52.
- 579 Hüttenbrink, K.B., 1988b. Die Mechanik der Gehörknöchelchenkette bei statischen Drucken.
580 II: Behinderte Gelenkfunktion und operative Kettenkonstruktion. Laryngol. Rhinol. Otol. 67,
581 100-105.
- 582 Hüttenbrink, K.B., 1997. The middle ear as a pressure receptor. Middle ear mechanics in
583 research and otosurgery. In: Hüttenbrink, K.B. (ed) Proc. Internat. Workshop, Dresden, 1996

584 Sep 19–22. Dept. Oto-rhinolaryngol., Univ. Hosp. Carl Gustav Carus, Dresden Univ.
585 Technology. 15–20.

586 Hüttenbrink, K.B., Pfautsch, M., 1987. Die Gelenke der Gehörknöchelchen im
587 rasterelektronen-mikroskopischen Bild. *Laryngol. Rhinol. Otol.* 66 (4), 176-179.

588 Kirikae, I., 1960. The Structure and Function of the Middle Ear. The University of Tokyo
589 Press.

590 Kobrak, H.G., 1959. The Middle Ear. University of Chicago Press.

591 Lauxmann, M., Eiber, A., Heckeler, C., Ihrle, S., Chatzimichalis, M., Huber, A.M., Sim, J.H.,
592 2012. In-plane motion of the stapes in human ears. *J. Acoust. Soc. Am.* 132 (5), 3280-3291.

593 Mach, E., Kessel, J., 1874. Beiträge zur Topographie und Mechanik des Mittelohres. *Sitz. ber.*
594 *Kais. Akad. Wiss. Math. Nat. wiss. Kl.* 3, 221-245.

595 Marquet, J., 1981. The incudo-malleal joint. *J. Laryngol. Otol.* 95, 543-565.

596 Nakajima, H.H., Ravicz, M.E., Merchant, S.N., Peake, W.T., Rosowski, J.J., 2005.
597 Experimental ossicular fixations and the middle ear's response to sound: evidence for a
598 flexible ossicular chain. *Hear. Res.* 204 (1-2), 60-77.

599 Offergeld, C.F.E., Hüttenbrink, K.B., Zahnert, T., Hoffmann, G., 2000. Experimental
600 investigations of ossicular joint ankylosis. In: Rosowski, J.J. and Merchant, S.N. (eds.), *The*
601 *function and mechanics of normal, diseased and reconstructed middle ears.* Kurger
602 Publication, The Hague, The Netherlands, 177-186.

603 Offergeld, C.F.E., Lasurashvili, N., Bornitz, M., Beleites, T., Zahnert, T., 2007. Experimental
604 investigations on the functional effect of ossicular joint fixation. In: Huber, A. and Eiber, A.
605 (eds.), *The 4th Symposium on Middle Ear Mechanics in Research and Otolaryngology.* World
606 Scientific Publishing, Singapore. 102-108.

607 Onchi, Y., 1961. Mechanism of the middle ear. *J. Acoust. Soc. Am.* 33, 794-805.

608 Politzer A, 1873. Zur physiologischen Akustik und deren Anwendung auf die Pathologie des
609 Gehörorgans. *Arch Ohrenheilkd.* 6, 35-44.

610 Politzer, A., 1884. *Traité des Maladies de l'Oreille.* Paris, ed. Octave Doin.

611 Puria, S, Steele, C.R., 2010. Tympanic-membrane and malleus-incus-complex co-adaptions
612 for high-frequency hearing in mammals. *Hear. Res.* 263, 183-190.

613 Rosowski, J.J., Davis, P.J., Merchant, S.N., Donahue, K.M., Coltrera, M.D., 1990. Cadaver
614 middle ears as models for living ears: comparisons of middle-ear input immittance. *Ann. Otol.*
615 *Rhinol. Laryngol.* 99, 403–412.

616 Savić, D., Djerić, D., 1988. Histopathological characteristics of degenerative modifications of
617 the incudomalleolar joint. *Ann Otolaryngol Chir Cervicofac.* 105, 203-6.

618 Schön, F., Müller, J., 1999. Measurements of ossicular vibrations in the middle ear. *Audiol.*
619 *Neurootol.* 4 (3-4), 142-149.

620 Schuknecht, H.F., 1974. *Pathology of the ear.* Cambridge, Mass.: Harvard University Press.

621 Sim, J.H., Chatzimichalis, M., Lauxmann, M., Rösli, C., Eiber, A., Huber, A.M., 2010.
622 Complex stapes motions in human ears. *J Assoc Res Otolaryngol.* 11 (3), 329-341.

623 Sim, J.H., Chatzimichalis, M., Rösli, C., Laske, R.D., Huber, A.M., 2012. Objective
624 assessment of stapedotomy surgery from round window motion measurement. *Ear & Hearing*.
625 33 (5), 24-31.

626 Sim, J.H., Puria, S., 2008. Soft tissue morphometry of the malleus-incus complex from micro-
627 CT imaging. *J Assoc Res Otolaryngol*. 9, 5-21.

628 Sim, J.H., Puria, S., Steele, C.R., 2004. Three-dimensional measurement and analysis of the
629 isolated malleus-incus complex. In: Gyo K and Wada H (eds.), *The 3rd International*
630 *Symposium on Middle Ear Mechanics in Research and Otology*. World Scientific Publishing,
631 Singapore. 61-67.

632 Sim J.H., Rösli C., Chatzimichalis M., Eiber A. and Huber A.M., Characterization of stapes
633 anatomy: investigation of human and guinea pig, *J. Assoc. Res. Otolaryngol*. 14 (2), 2013,
634 159-73.

635 Stuhlman, O., 1937. The nonlinear transmission characteristics of the auditory ossicles. *J.*
636 *Acoust. Soc. Am*. 9, 119-128.

637 Tonndorf, J., Khanna, S.M., 1967. Some properties of sound transmission in the middle and
638 outer ears of cats. *J. Acoust. Soc. Am*. 41, 513–521.

639 Tonndorf, J., Khanna, S.M., 1968. Submicroscopic displacement amplitudes of the tympanic
640 membrane (cat) measured by a Laser interferometer. *J. Acoust. Soc. Amer*. 44, 1546-1554.

641 Voss, S.E., Rosowski J.J., Merchant, S.N., Peake, W.T., 2000. Acoustic responses of the
642 human middle ear. *Hear. Res*. 150, 43-69.

643 Willi, U.B., 2003. Middle-ear mechanics: the dynamic behavior of the incudo-malleolar joint
644 and its role during the transmission of sound. *Doctoral Thesis in Mathematics and Natural*
645 *Science*. University of Zurich, Zurich.

646 Willi, U.B., Ferrazzini, M.A., Huber, A.M., 2002. The incudo- malleolar joint and sound
647 transmission losses. *Hear. Res*. 174 (1-2), 32–44.

648 Zwislocki, J., Feldman. A.S., 1963. Post-mortem acoustic impedance of human ears. *J.*
649 *Acoust. Soc. Am*. 35, 104- 107.

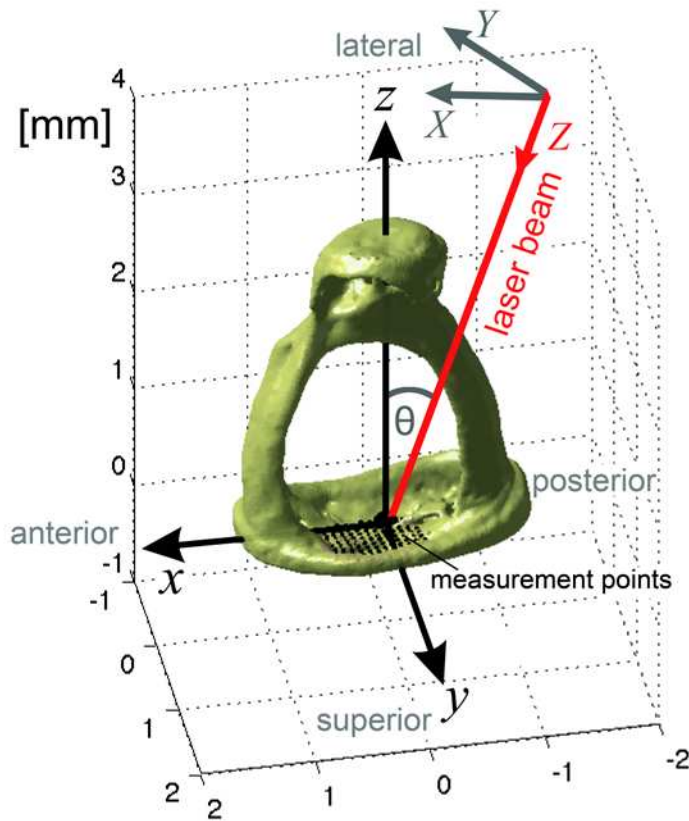


Fig. 1 SLDV measurement frame (XYZ coordinate system) and footplate-fixed anatomical frame (xyz coordinate system) for the right ear (right-handed frame system). In the SLDV measurement frame, the XYZ coordinate system was set such that the laser beam was along the Z direction and the XY plane was normal to the laser beam. In the footplate-fixed anatomical frame, the xy -plane was fitted to the median surface of the stapes footplate, and the origin at the centroid of the median surface. The anterior direction was set as the positive x -direction, the superior direction as the positive y -direction, and lateral direction as the positive z -direction. The angle θ between the laser beam direction (i.e., Z axis of SLDV frame) and the z axis of the anatomical frame was $34 \pm 11^\circ$.

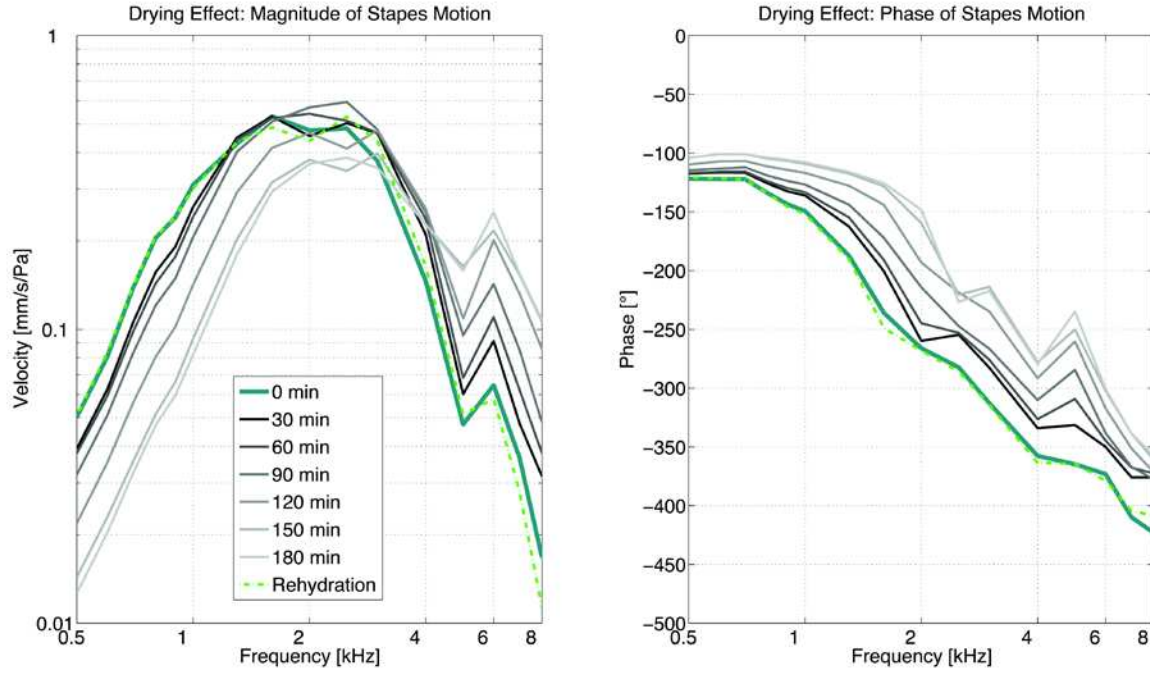


Fig. 2 Changes in the magnitudes (left) and phases (right) of motions of the stapes footplate (center) with drying. After the sample was dried for 180 minutes, it was rehydrated by immersion in saline solution.

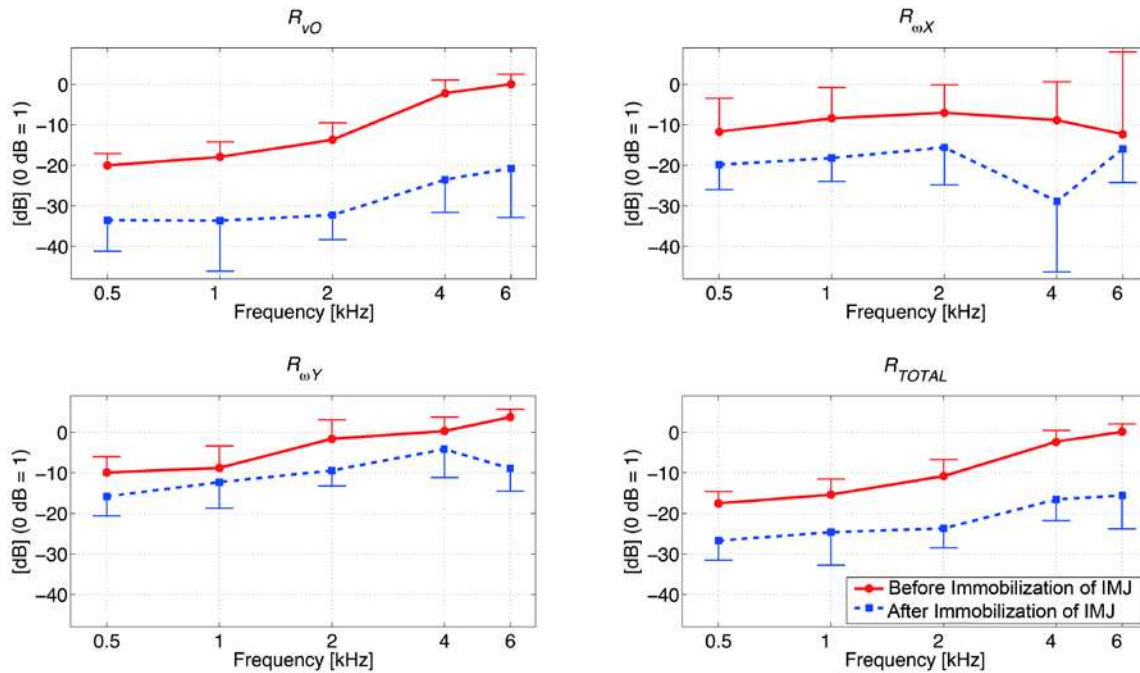
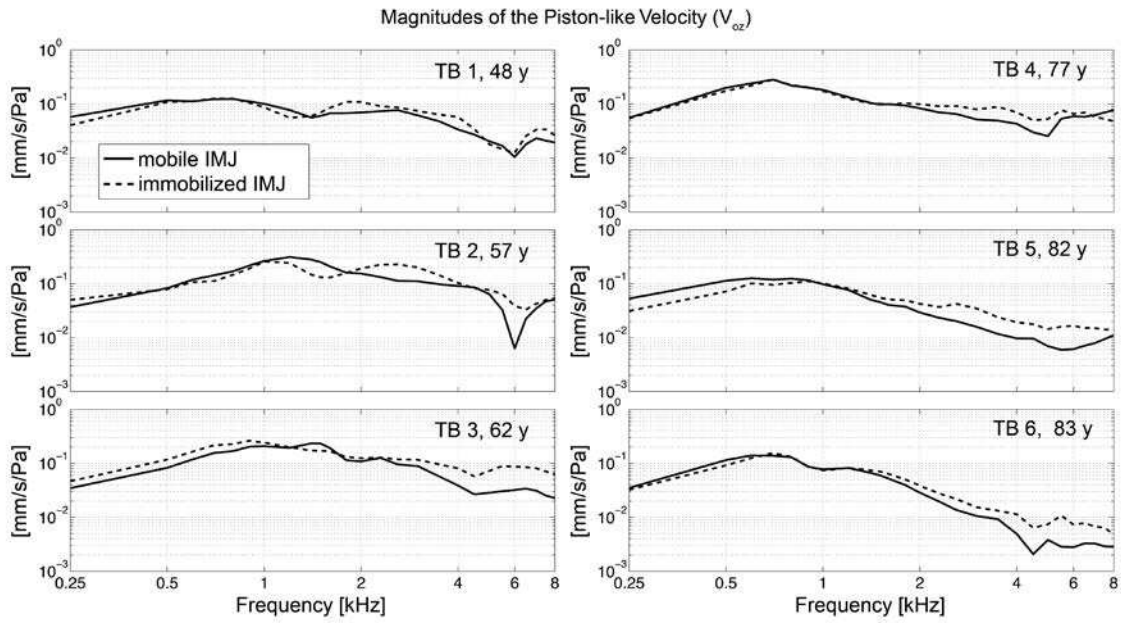


Fig. 3 Relative motion between the malleus and incus represented by the ratios of the relative motion components to the corresponding motion components of the malleus and incus, before IMJ was immobilized (solid) and after the IMJ was immobilized (dashed). The relative motion ratios for V_O (R_{vO} , left upper), ω_X ($R_{\omega X}$, right upper), ω_Y ($R_{\omega Y}$, left below), and average with the ratio components weighted by portions of the corresponding motion components (R_{TOTAL} , right below). The ratio of 1 (= 0 dB) indicates that the magnitude of the relative motion component is the same as the average magnitude of the corresponding malleus motion component and the corresponding incus motuion component.

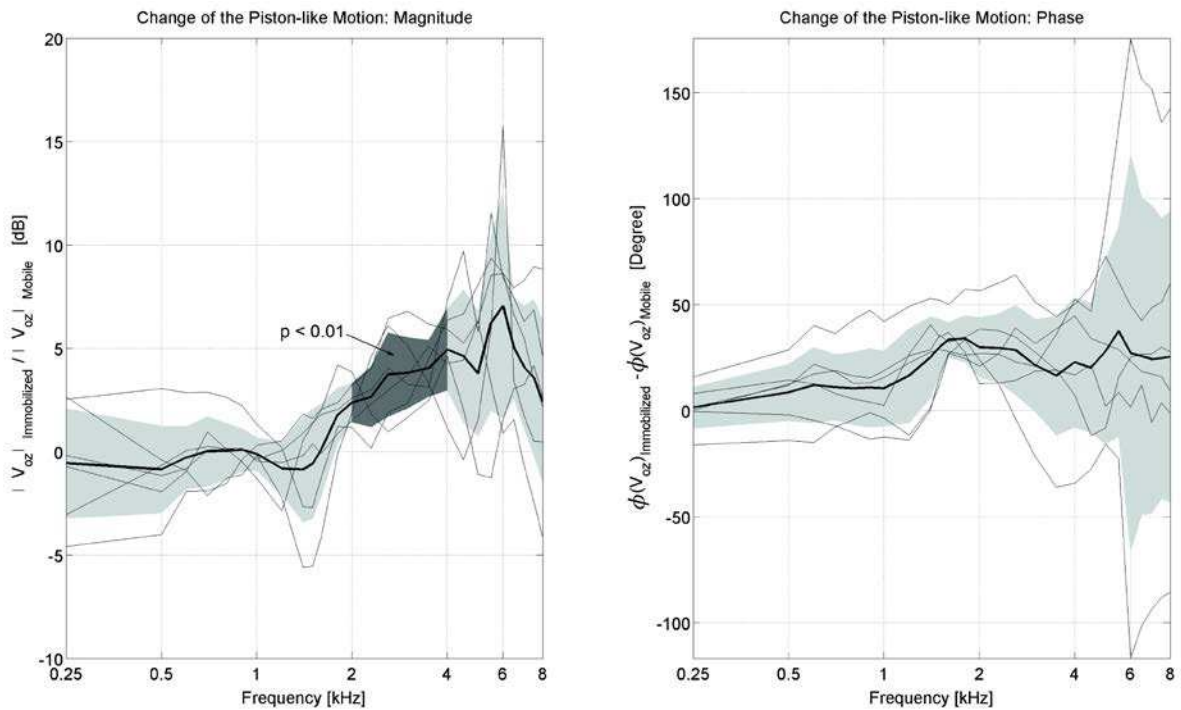
677



678

679 **Fig. 4** Magnitudes of the translational motions of the footplate center along the z -axis (i.e.,
680 piston-like motions, V_{oz}) normalized by the ear canal pressure, before (solid) and after
681 (dashed) the IMJ is immobilized.

682



683

684 **Fig. 5** Change of the translational motion with immobilized IMJ relative to the translational
685 motion with mobile IMJ. Relative magnitude ratios (left) and relative phase difference (right)
686 with the mean values (thick lines) and standard deviations (shaded). Prominent differences in
687 magnitude between the mobile and immobilized conditions of the IMJ are shown as shaded
688 with dark gray (2- 4 kHz and 5.5 kHz, $p < 0.01$ with paired t -test).

689

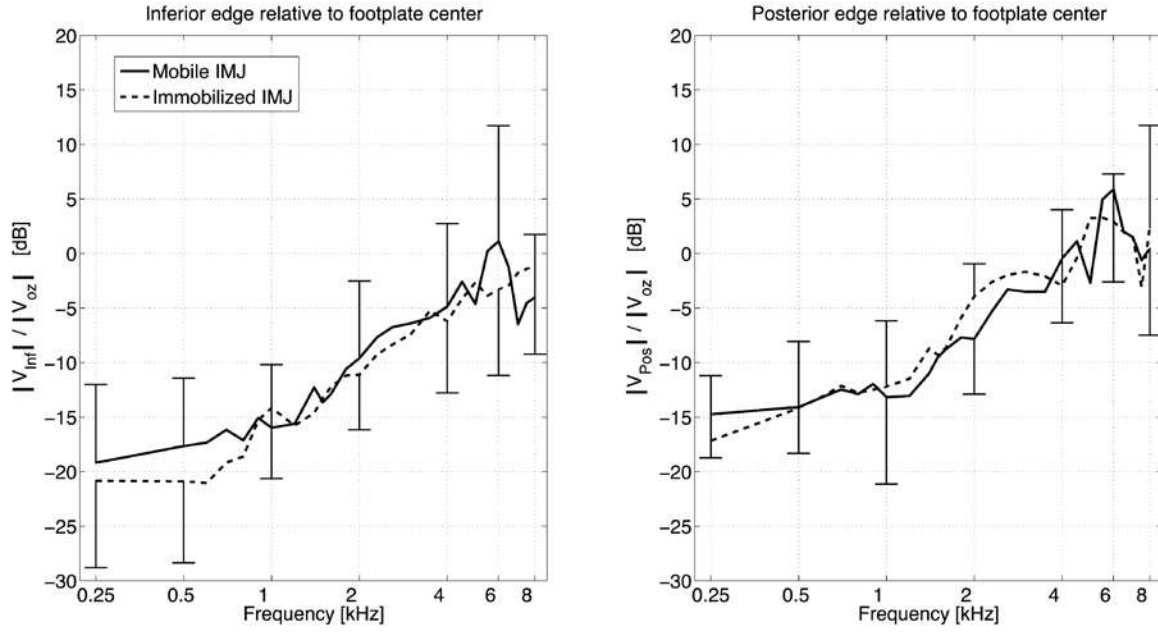


Fig. 6 Relative magnitudes of the edge velocities generated by the rocking-like motions (i.e., two rotational motions along the long and short axes of the footplate) with respect to the piston-like motion (i.e., the footplate-center velocity in the z -direction), before (solid) and after (dashed) the IMJ immobilization. The inferior-edge velocity due to the rocking-like motion of the footplate along the long axis (left), and the posterior-edge velocity due to the rocking-like motion of the footplate along the short axis (right).